Cellular and Molecular Bioengineering, Vol. 14, No. 5, October 2021 *(© 2021)* pp. 459–469
https://doi.org/10.1007/s12195-021-00688-7

2021 CMBE Young Innovators

Vesicle-Based Sensors for Extracellular Potassium Detection

MARGRETHE A. BOYD,[1] ANNA M. DAVIS,[1] NORA R. CHAMBERS,[1] PETER TRAN,[3] ARTHUR PRINDLE,[2,3,4] and NEHA P. KAMAT [1,2]

[1]Department of Biomedical Engineering, McCormick School of Engineering, Northwestern University, Evanston, IL 60208, USA; [2]Center for Synthetic Biology, McCormick School of Engineering, Northwestern University, Evanston, IL 60208, USA; [3]Department of Chemical and Biological Engineering, McCormick School of Engineering, Northwestern University, Evanston, IL 60208, USA; and [4]Department of Biochemistry and Molecular Genetics, Feinberg School of Medicine, Northwestern University, Chicago, IL 60611, USA

(Received 22 February 2021; accepted 7 July 2021; published online 10 August 2021)

Associate Editor Michael R. King oversaw the review of this article.

Abstract
Introduction—The design of sensors that can detect biological ions *in situ* remains challenging. While many fluorescent indicators exist that can provide a fast, easy readout, they are often nonspecific, particularly to ions with similar charge states. To address this issue, we developed a vesicle-based sensor that harnesses membrane channels to gate access of potassium (K^+) ions to an encapsulated fluorescent indicator.
Methods—We assembled phospholipid vesicles that incorporated valinomycin, a K^+ specific membrane transporter, and that encapsulated benzofuran isophthalate (PBFI), a K^+ sensitive dye that nonspecifically fluoresces in the presence of other ions, like sodium (Na^+). The specificity, kinetics, and reversibility of encapsulated PBFI fluorescence was determined in a plate reader and fluorimeter. The sensors were then added to *E. coli* bacterial cultures to evaluate K^+ levels in media as a function of cell density.
Results—Vesicle sensors significantly improved specificity of K^+ detection in the presence of a competing monovalent ion, sodium (Na^+), and a divalent cation, calcium (Ca^{2+}), relative to controls where the dye was free in solution. The sensor was able to report both increases and decreases in K^+ concentration. Finally, we observed our vesicle sensors could detect changes in K^+ concentration in bacterial cultures.
Conclusion—Our data present a new platform for extracellular ion detection that harnesses ion-specific membrane transporters to improve the specificity of ion detection. By changing the membrane transporter and encapsulated sensor, our approach should be broadly useful for designing biological sensors that detect an array of biological analytes in traditionally hard-to-monitor environments.

Keywords—Membrane, Biosensing, Liposome, Ionophore, Fluorescence.

INTRODUCTION

Potassium ions (K^+) are one of the most abundant cations present in intracellular fluid, playing a critical role in maintaining cell potential and excitability, cell volume, and acid-base balance.[11,28] As such, the concentration of this ion both in and outside of the cell affects a wide variety of cellular processes in living organisms, from driving neuronal activity to coordinating communication between bacteria in biofilms.[29,37] In humans, irregularities in extracellular K^+ levels contribute to a range of pathologies, including cardiovascular disease, immunological diseases, and some cancers.[6,9,10,26,32] In addition, disruption of K^+ channels in bacteria can abolish the coordinated growth of bacterial communities.[29] Despite the critical role of K^+ ions in a wide range of cellular behaviors, the detection, quantification and monitoring of K^+ remains difficult in a number of contexts. In particular, ion-sensitive electrodes, the state-of-the-art method to quantify K^+ in biological samples, are invasive and unable to report the spatiotemporal dynamics of K^+ variations in living systems.[1,2,36] While we continue to learn about the role of K^+ in driving cellular function, this limitation in our abilities to measure the concentrations of K^+ both intra- and extracellularly subsequently limits our

Address correspondence to Neha P. Kamat, Department of Biomedical Engineering, McCormick School of Engineering, Northwestern University, Evanston, IL 60208, USA. Electronic mail: nkamat@northwestern.edu

1865-5025/21/1000-0459/0 © 2021 Biomedical Engineering Society

understanding of how these fluctuations may accompany healthy or irregular cellular and organelle function. For this reason, the design of fluorescent potassium sensors that can optically report variations in extracellular K^+ concentrations *in situ* would be greatly valuable.

Several optical probes that respond to K^+ ions have been developed to date.[12,23,27,31,38] Unfortunately, these small-molecule probes can be unable to selectively measure K^+ ions when in the presence of other ions—particularly ions with similar charge states, such as Na^+[22,30]—and can be difficult to deploy in biological studies due to technological limitations in cell loading or toxicity.[2,16,18] One commonly used, commercially-available K^+ probe is potassium-binding benzofuran isophthalate (PBFI),[22,23] which has been used for the intracellular quantification of K^+.[8,13,14] Cells establish a significant K^+/Na^+ gradient in order to maintain proper membrane potential, with ~150 mM KCl and 10 mM NaCl concentrations maintained intracellularly.[13,31] Extracellularly, however, these concentrations are inverted, with high Na^+ and K^+ concentrations as low as 3–5 mM.[6] PBFI exhibits poor selectivity against Na^+, with only 1.5x higher selectivity for K^+ than Na^+, which limits its use to intracellular applications where K^+ concentrations far outweigh the concentration of Na^+.[13] Similar limitations are encountered with other optical probes, including Asante Potassium Green and its variants.[30] Without the ability to control for the effects of other cations, this lack of specificity in ion detection ultimately limits the accuracy of K^+ sensing by certain optical sensors in many biological environments.

One strategy to improve the specificity of small-molecule ion indicators is to selectively gate which ions are able to access the indicator. Previous approaches have incorporated optical ion indicators within silica-based nanoparticles, however, the assembly and characterization of these sensor platforms rely on multiple coating and characterization steps and may not be easily transferrable to other ion types.[17,18] An alternative approach is to encapsulate these optical indicators within bilayer membranes, which are easily assembled and can incorporate a wide variety of naturally-derived or synthetic components.[3] Lipid vesicles formed through the self-assembly of phospholipids can encapsulate water soluble cargo within a semipermeable barrier.[3,24] Mimicking the structure of cellular membranes, these particles can be co-assembled with peptides and proteins that selectively interact with ions to enable their passage across a membrane in order to interact with an encapsulated ion indicator.[19,33] Valinomycin, an ionophore, is one such molecule that selectively transports alkali metals through both biological and synthetic membranes.[25] This cyclic peptide can form an ion-peptide complex with select metallic cations, including K^+, Rb^+, and Cs^+, but the cavity of the valinomycin ring is incompatible with Na^+.[34] As a result, valinomycin selectively transports K^+ over Na^+ ions across bilayer membranes.

Here, we present a new approach to selectively detect K^+ in the presence of Na^+ by developing a vesicle-based nanosensor. To achieve this goal, we assemble lipid vesicle membranes encapsulating the K^+ indicator PBFI in the vesicle lumen, and incorporate valinomycin into the vesicle membranes (Fig. 1). We show that this nanosensor can selectively detect K^+ in the presence of other important biological cations, and demonstrate the nanosensor can detect changes in extracellular K^+ concentration in bacterial cultures. The approach presented here should be extendable to a range of ions, which can be customized by altering the ion transporter and ion indicator. As a result, we expect our methods will enable a new generation of ion sensors that will reveal new information about extracellular ion variations during normal and pathological functions.

RESULTS

Spectral Characterization of PBFI in Solution

We first characterized the fluorescence of free PBFI in solution as a function of KCl concentration to verify this relationship in our selected buffer. PBFI was mixed with a Tris buffer (pH 7) containing increasing concentrations of KCl and the emission of PBFI at 505 nm was monitored upon excitation with light ranging from 320 to 400 nm, as previously described.[22] As expected, emission maxima were detected at an excitation wavelength of 340 nm, and emission intensity increased in response to both increasing KCl and NaCl concentrations (Figs. 2a and 2b). Spectral shifts in PBFI fluorescence were subsequently reported ratiometrically, where the fluorescence intensity ratio was determined at the emission maximum of 505 nm when excited at 340/380 nm.[22] Using this metric, we then measured the PBFI fluorescence intensity ratio as a function of monovalent ion identity and concentration, as well as the response to a combination of ions (Fig. 2d). We observed that PBFI responds to both ions and appears to saturate in signal at approximately 50 mM (Figs. 2b and 2d). In the presence of a combination of Na^+ and K^+ with a constant total salt concentration, however, no change in PBFI ratio is observed even as K^+ concentration increases; this result demonstrates the lack of indicator specificity and an inability to distinguish K^+ from Na^+ ions when free in solution (Fig. 2d).

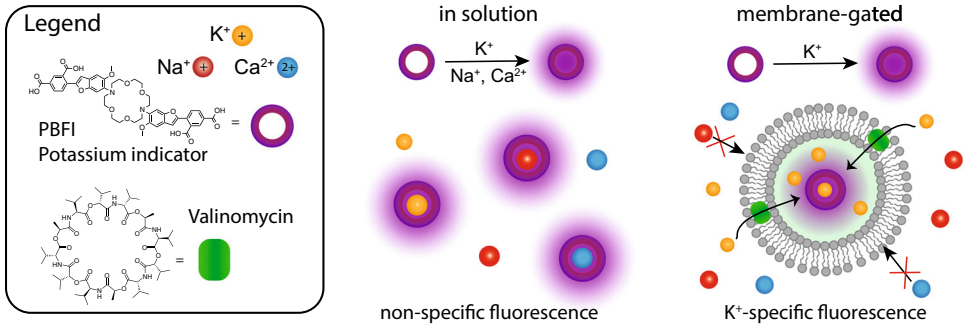

FIGURE 1. Design of the vesicle-based K^+ nanosensor. PBFI, a commonly used indicator of K^+ ions, fluoresces in the presence of K^+ as well as other ions, such as Na^+ and Ca^{2+}. In solution, PBFI fluorescence due to K^+ binding is indistinguishable from PBFI fluorescence due to Na^+ and Ca^{2+} binding. Membrane gating provides a route to selectively exclude ions from binding to PBFI. By encapsulating PBFI in lipid vesicles that contain valinomycin, a cyclic peptide that selectively transports K^+ ions across bilayer membranes, K^+ can diffuse in and out of the vesicle. Once inside the vesicle nanosensor, K^+ can bind PBFI to generate an optically detectable fluorescence shift. By contrast, Na^+ and Ca^{2+} ions are excluded from the vesicle interior and their presence will not be reported.

Encapsulation in Lipid Vesicles Increases the Specificity of PBFI

We hypothesized that one strategy to address the nonspecific response of PBFI to various cations could be to introduce a secondary molecular gating method through the incorporation of bilayer membranes. Ionic balances must be constantly maintained in living organisms, and as such, a number of naturally-occurring membrane transporters exist for various ions.[33] One such transporter, a bacterially-derived ionophore called valinomycin, specifically transports K^+ ions across membranes.[34] We hypothesized that encapsulating PBFI within valinomycin-containing bilayer vesicles would allow for a specific response to K^+ over other ions. To assess this, lipid vesicles encapsulating PBFI were assembled from thin film hydration techniques using 1,2-dioleoyl-sn-glycero-3-phosphocholine (DOPC) lipids, extruded to a size of 100 nm, and purified to remove unencapsulated dye. The average vesicle diameter was measured using dynamic light scattering and was found to be 99.32 nm, with a polydispersity index of 0.151. To incorporate valinomycin into vesicle membranes, we solubilized the ionophore in DMSO and added it to preformed, purified vesicles. Vehicle controls were prepared by adding the same final volume of DMSO to vesicles in the absence of valinomycin. We expected our resulting vesicle-based nanosensor with incorporated valinomycin would allow us to spatially segregate PBFI from environmental ions and gate transport of K^+ ions to the vesicle interior (Fig. 1).

Once assembled, we first focused on determining the specificity of these nanosensors to K^+ over Na^+ ions (Fig. 3a). The PBFI fluorescence ratio was measured as a function of valinomycin concentration across varying salt conditions (Figs. 3b–3d). We examined three K^+/Na^+ conditions in which we increased K^+ concentrations in the presence of Na^+ or increased only K^+ or Na^+ in the absence of the other ion. When vesicles were incubated in the presence of both K^+ and Na^+ with a constant total salt concentration of 100 mM (i.e. increasing $[K^+]$ paired with decreasing $[Na^+]$) (Fig. 3a), the valinomycin-containing vesicles demonstrated a fluorescent response specific to increasing $[K^+]$, while vesicles without ionophore did not exhibit any changes in fluorescence. These results indicate that valinomycin is necessary for the transport of K^+ across the membrane, and that these nanosensors respond specifically to $[K^+]$ rather than the total salt concentration.

Next, nanosensors were incubated with K^+ or Na^+ separately. In the presence of increasing $[K^+]$ alone, PBFI fluorescence in vesicles with valinomycin increased to a similar degree compared to vesicles in the presence of both K^+ and Na^+ (Fig. 3c). In comparison, vesicles incubated with only Na^+ exhibited minimal fluorescent response, indicating that Na^+ is not able to pass through valinomycin or the vesicle membrane to interact with encapsulated PBFI dye (Fig. 3d). A small amount of nonspecific leakage of Na^+ into vesicles was observed at high salt concentrations ($[Na^+] \geq 75$ mM), as expected in highly hypertonic conditions. Importantly, the magnitude of the fluorescent output of the sensor when K^+ is the only ion present (Fig. 3d) is nearly identical to the fluorescent output when both K^+ and Na^+ are present (Fig. 3b), further indicating that nanosensors are sensitive to and specific for K^+ even when Na^+ is present.

We then assessed the specificity of these nanosensors in the presence of an expanded range of biologically relevant divalent cations, specifically Ca^{2+} and Mg^{2+} (Fig. 3e). To compare PBFI responses between conditions where PBFI was encapsulated or free in solution, we kept the total PBFI concentration in samples

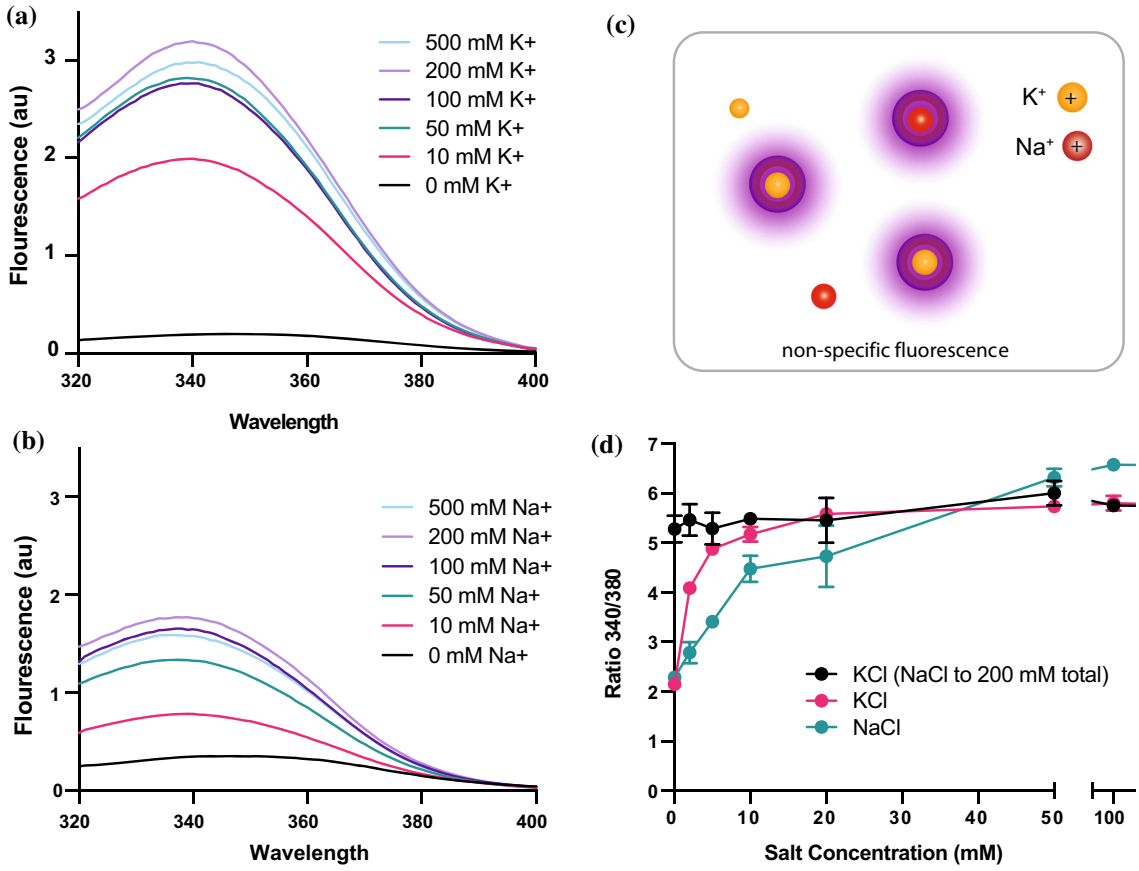

FIGURE 2. Spectral characterization of the PBFI indicator. (a) Emission spectra of PBFI in solution as a function of K^+ concentration and (b) Na^+ concentration. (c) A schematic of these studies shows that, in solution, a variety of ions are expected to interact with PBFI and shift the fluorescence of the indicator. (d) The fluorescence intensity ratio of PBFI emission at 505 nm when excited at 340 and 380 nm is reported as a function of salt concentration for KCl and/or NaCl. This reported 340/380 intensity ratio is standard to assess K^+ concentrations when using PBFI. *N* = 3, error bars represent standard deviation.

constant. To do this, we prepared vesicles containing PBFI and measured the fluorescence ratio in the presence of 50 mM total salt when vesicles were intact or lysed with a detergent, TritonX-100. As an additional control, we compared these results to PBFI in solution at the estimated final concentration of PBFI following vesicle purification. The fluorescent responses of lysed vesicles and free dye in the presence of various cations show off-target responses to both Na^+ and Ca^{2+} when vesicle membranes are disrupted or are not present. In contrast, intact vesicles containing valinomycin exhibit fluorescent responses to K^+ specifically. While the overall magnitude of fluorescence was reduced in vesicles compared to lysed vesicles or free dye (Fig. S2), when compared to the maximum K^+ signal for a given encapsulation condition, the specificity to K^+ over Na^+ and Ca^{2+} is significantly improved (Fig. 3e). Taken together, these results demonstrate the ability of these nanosensors to modulate interactions between encapsulated PBFI and the surrounding environment, allowing specific detection of K^+ concentrations—even in the presence of other cations.

The responses of our K^+ nanosensor in all salt conditions were observed to be limited to vesicles with intact membranes and incorporated valinomycin ionophores. Vesicles remained stable across the range of salt concentrations assessed (Fig. S1, Fig. S3), further indicating that improved specificity to K^+ occurs through gated entry into the vesicle lumen. Additionally, in this set of stability studies we observed that valinomycin concentrations up to 0.2 mol% maintained K^+ specificity, and therefore chose to proceed with our studies using 0.2 mol% valinomycin in vesicles. Further, we verified that the quantity of DMSO used to solubilize valinomycin does not lead to significant nonspecific leakage of PBFI or transport of ions into vesicle membranes, as indicated by vehicle controls.

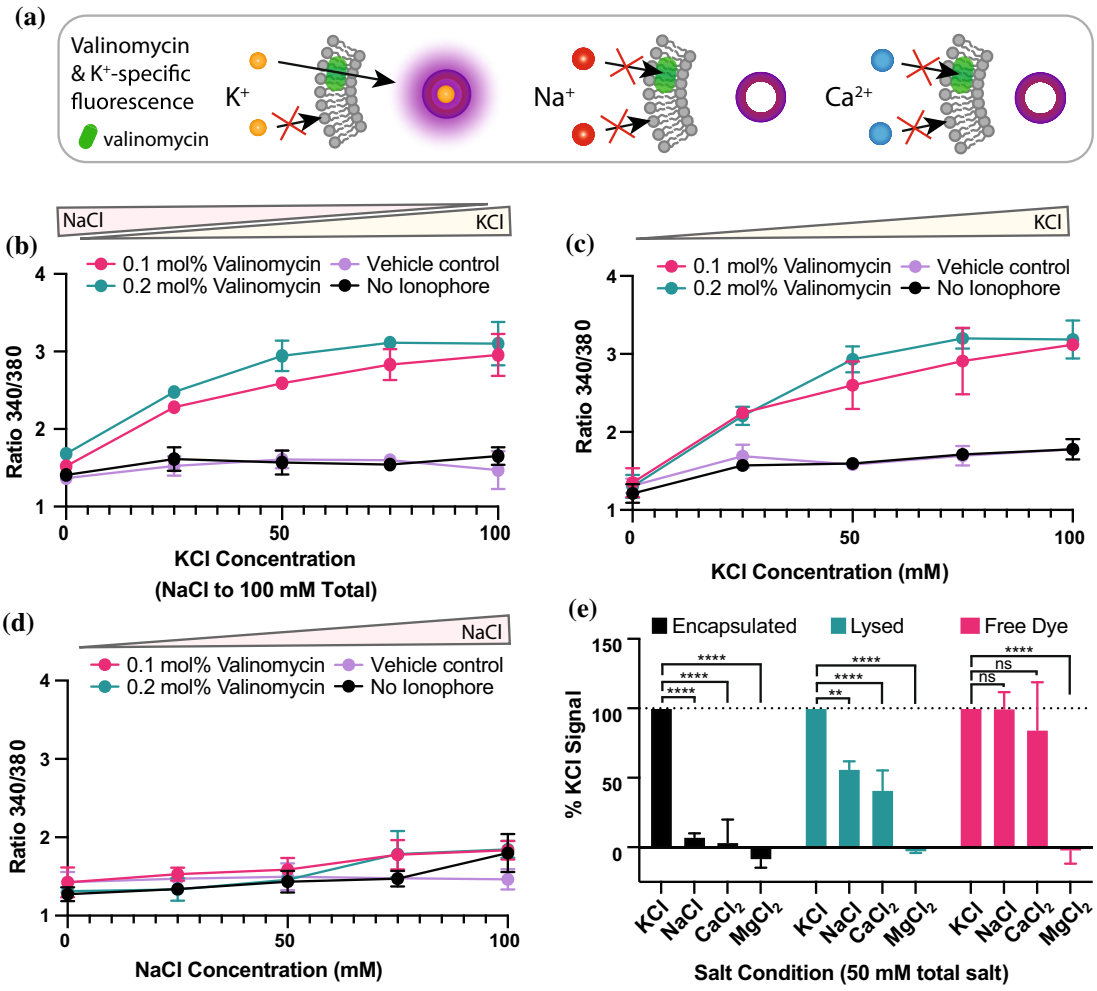

FIGURE 3. Encapsulation of PBFI with valinomycin as a membrane gate improves specificity to K^+. (a) Schematic illustrating how membrane gating with valinomycin results in K^+-specific access to encapsulated PBFI dye. (b) Vesicles with either 0.1 mol% or 0.2 mol% valinomycin exhibit a significant increase in PBFI ratio as K^+ concentration increases compared to respective control vesicles, even when Na^+ is present at a total salt concentration of 100 mM ($p \leq 0.0001$, $[K^+] > 0$ mM). Vesicles without ionophore or with DMSO only (vehicle controls) do not exhibit a response, indicating that increases in PBFI ratio are due to cross-membrane transport of K^+ by valinomycin. (c) Vesicles with valinomycin exhibit significant increases in PBFI ratio as K^+ concentration increases compared to respective control vesicles ($p \leq 0.0001$, $[K^+] > 0$ mM), which do not exhibit a significant response. (d) Vesicles with and without valinomycin do not exhibit significant changes in fluorescence as Na^+ concentrations increase up to 50 mM (samples are not significantly different when $[Na^+] < 75$ mM), with slight nonspecific leakage leading to increased PBFI fluorescence at high Na^+ concentrations compared to respective controls. Samples are significantly different ($p \leq 0.05$) when $[Na^+] = 100$ mM. (e) Fluorescence ratios reported as a percentage of the maximum KCl signal observed for either PBFI encapsulated in vesicles, PBFI released into solution through vesicle lysis, or free PBFI in solution. In the absence of intact membranes, PBFI reports a higher fluorescence ratio in the presence of NaCl and $CaCl_2$ in addition to KCl. $N = 3$, error bars represent standard deviation. ****$p \leq 0.0001$, **$p \leq 0.01$, *$p \leq 0.05$, nonsignificant (ns) $p > 0.05$; p-values generated using a Two-Way ANOVA and Tukey's Multiple Comparisons Test.

Kinetics and Reversibility of K^+ Nanosensors

Having demonstrated that the encapsulation of PBFI with valinomycin-based membrane gating improves the specificity of vesicle nanosensors to K^+, we next wanted to explore the response of these nanosensors to changing KCl concentrations over time. While membrane gating reduces the ability of off-target cations to access encapsulated PBFI, it also creates a barrier between the dye and free K^+ ions. To determine the effect of this spatial segregation on sensing kinetics, we monitored the PBFI response in nanosensors over time following the external addition of 50 mM KCl. Intact nanosensors with 0.2 mol% valinomycin exhibited increasing PBFI fluorescence ratios over time, with a significant difference in signal observable within 10 min (Fig 4a). PBFI signals were observed to plateau after 1 h (Fig. 4b); these results were fit to a one-phase association model, with PBFI fluorescence described as: $Ratio340/380 = 1.86 + 0.42\left(1 - e^{0.04t}\right)$ ($R^2 = 0.84$), yielding a rate constant of

0.04 min^{-1}. No fluorescence changes were observed in vehicle controls, and vesicles lysed with TritonX-100 exhibited significantly higher PBFI ratios than either intact vesicle condition (Fig. 4a). High PBFI ratios following vesicle lysis indicate that valinomycin-gated vesicles remained intact during salt incubation (Fig. 4b). While these results indicate that membrane gating does introduce a physical barrier to sensing, thereby increasing the time it takes for nanosensors to reach maximum signal, increases in PBFI ratios were clearly observable on shorter timescales. It is important to note that the maximum increase in PBFI fluorescence is only about 2-fold, which may make the determination of a specific K^+ concentration difficult without sample-specific calibration. Despite this, these nanosensors allow improved comparison between

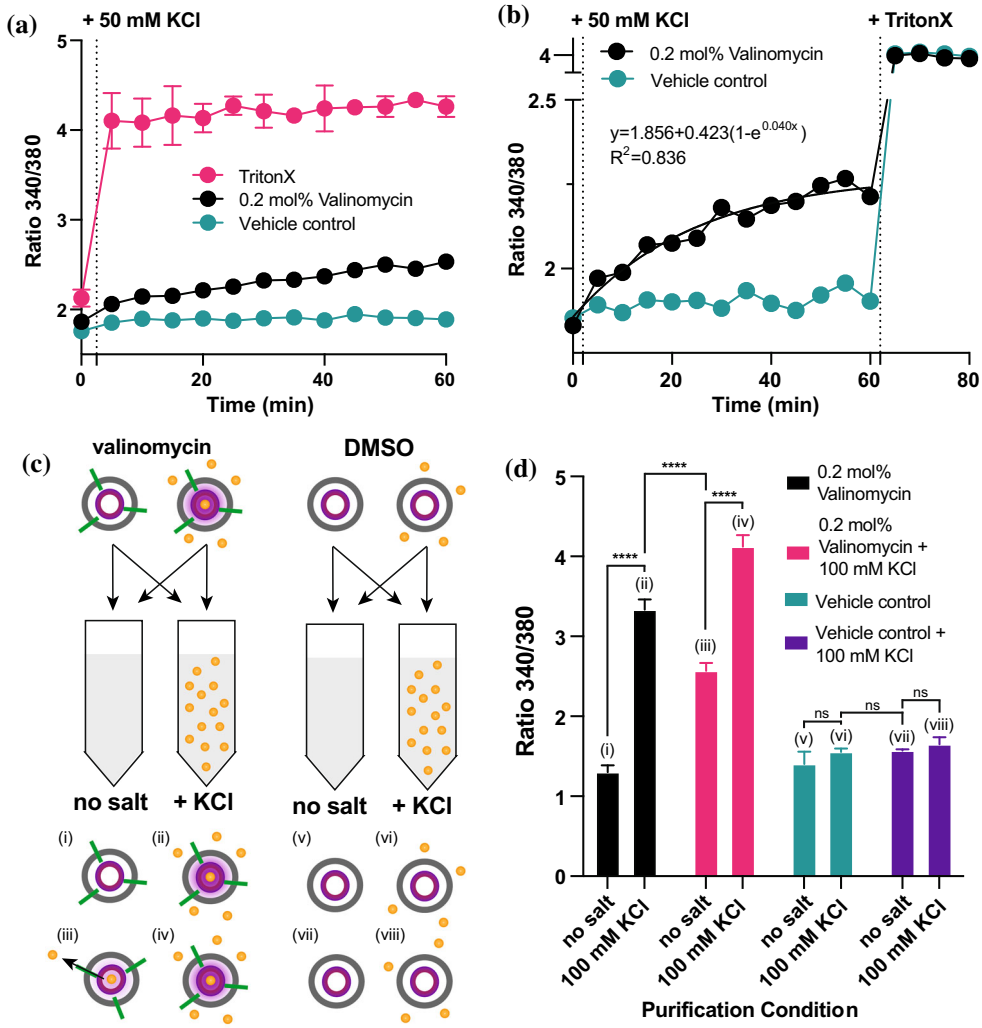

FIGURE 4. Response of vesicle sensors to changing salt conditions over time. (a) PBFI fluorescence in vesicles with valinomycin in the membrane increases over time following 50 mM KCl addition to surrounding buffer. Fluorescence does not change in corresponding vehicle controls, indicating that increasing PBFI ratios in vesicles are due to valinomycin-specific transport of K^+. 0.2% valinomycin vesicles exhibit a significantly higher PBFI ratio than vehicle controls within 10 minutes ($p \leq 0.05$), and high PBFI ratios in TritonX-lysed controls indicate that valinomycin-containing vesicles remained intact. (b) PBFI ratios in valinomycin-containing vesicles fitted to a one-phase association model (equation shown on graph). After lysis with TritonX, an increase in PBFI ratio indicates that vesicles remained intact following KCl addition. (c) Schematic of reversibility assays. Four populations of vesicles were generated: with and without valinomycin and with and without 100 mM KCl. Each population was purified through two columns, resulting in eight final salt conditions. Numerals correspond to results in (d) and yellow circles represent potassium. (d) Vesicles incubated without KCl (black) show a significant increase in PBFI ratio when purified through SEC columns with 100 mM KCl in the running buffer, while vesicles incubated with 100 mM KCl (pink) show a significant reduction in PBFI ratio when purified through SEC columns without salt in the running buffer. Vesicles with and without pre-incubation in KCl show significantly higher PBFI ratios when purified with KCl in the running buffer compared to salt-free buffer. Vehicle control vesicles both with (purple) and without pre-incubation (green) show no significant difference in fluorescence following purification. $N = 3$, error bars represent standard deviation. ****$p \leq 0.0001$, ***$p \leq 0.001$, **$p \leq 0.01$, *$p \leq 0.05$, nonsignificant (ns) $p > 0.05$; p-values generated using a Two-Way ANOVA and Tukey's Multiple Comparisons Test.

samples, and could also be used as a binary sensor to indicate the presence or absence of K^+ above a given threshold. These effects could possibly be improved in the future by incorporating faster transport mechanisms, such as counter ion pores, or by increasing the amount of valinomycin in the membrane.

We also wondered whether the response of these nanosensors was reversible, and if the removal of salt from the surrounding environment would cause PBFI fluorescence to decrease. To assess this, we altered the running buffers used for size exclusion chromatography to add or remove salt from vesicle buffers. We first incubated unpurified nanosensors with or without 100 mM KCl for one hour, allowing them to saturate with K^+. We then purified them using running buffer both with and without 100 mM KCl, with some nanosensors experiencing addition of KCl during purification and others experiencing KCl removal, and allowed them to incubate in these new conditions for another hour. As expected, nanosensors incubated without KCl exhibited low PBFI ratios when purified without salt, whereas PBFI responses increased significantly when 100 mM KCl was introduced in the running buffer. In contrast, nanosensors incubated with saturating levels of KCl prior to purification exhibited a further increase in PBFI signal following purification with excess KCl, while the PBFI signal when purified without salt was decreased. Dye leakage assays indicated that nanosensors remain stable throughout the incubation and purification processes (Fig. S3). Importantly, the reduced signal observed in the preincubated-with-salt/purified-without-salt condition compared to the preincubated-without-salt/purified-with-salt condition indicates some degree of reversibility in the nanosensor signal in response to changing K^+ (Fig. 4c). We therefore expect these nanosensors could ultimately respond to dynamic salt conditions, increasing and decreasing fluorescence with changes in $[K^+]$ over time.

Assessing K^+ Nanosensors in Bacterial Cultures

Finally, we wanted to determine if these nanosensors could monitor K^+ concentrations in a biological context. Specifically, we wanted to assess whether nanosensors could detect changes in salt concentrations due to bacterial release or uptake. To accomplish this, we resuspended pelleted BL21 *Escherichia coli* grown in MSgg media into Tris buffer, and mixed bacteria with nanosensors (0.2 mol% valinomycin and vehicle control, 1 mM final concentration in Tris buffer) in fluorimeter cuvettes to three different optical densities. We monitored nanosensor fluorescence in the presence of increasing concentrations of bacteria without any salt for 30 min in order to assess any changes in fluorescence due to bacterial addition alone. We observed slightly decreased levels of baseline fluorescence as the concentration of bacteria increased, but variations were small and did not change over time (Fig. S4). We then added 150 mM NaCl and 50 mM KCl to each cuvette to generate a salt shock and monitored PBFI spectra for 1 h. To control for variations in baseline fluorescence due to increased optical density, final PBFI fluorescence in nanosensors was normalized to initial pre-salt values (Fig. 5c). In the presence of NaCl and KCl, we observed a significant decrease in the change in PBFI ratio as bacterial concentration increased (Fig. 5c), indicating a lower K^+ concentration detected by the nanosensors. We expect that this is due to NaCl creating a hyperosmotic shock, inducing the bacteria to take up K^+ from the surrounding buffer.[5,7,20,21,35] With a higher number of bacteria present, we expect that this uptake would have an overall greater effect on the bulk K^+ concentration.[15] A nonsignificant decrease in fluorescence was observed in vehicle controls, however this is consistent with nonspecific leakage observed in high salt conditions (Fig. S4). A similar decrease in nanosensor fluorescence was observed in studies monitoring K^+ in bacterial supernatant following incubation with increasing concentrations of bacteria, further supporting this hypothesis (Fig. S5)

We then imaged vesicles co-incubated with bacteria for 1 h to assess stability and localization. We were unable to assess the 380 nm excitation of PBFI and therefore the ratiometric response to K^+, however we observed the fluorescence of a vesicle membrane dye, Cy5.5-PE, co-localized with faint PBFI fluorescence at the 340 excitation, indicating vesicles remain intact in the presence of bacteria (Fig. 5b). Overall, these results indicate that these nanosensors are able to detect changes in K^+ concentrations in biological samples, even in the presence of high Na^+ concentrations. Moving forward, however, buffers may need to be optimized or matched for a given biological environment and sensor calibration may be required for diverse sample types. With these factors taken into account we expect these results could be expanded to other biological contexts, including samples from eukaryotic systems.

CONCLUSION

Here, we have demonstrated that the specificity of an optical K^+ indicator can be improved by spatially segregating the indicator from its surrounding environment and introducing molecularly-specific transporters to modulate its access to various ions. We observed that the encapsulation of PBFI dye in lipid

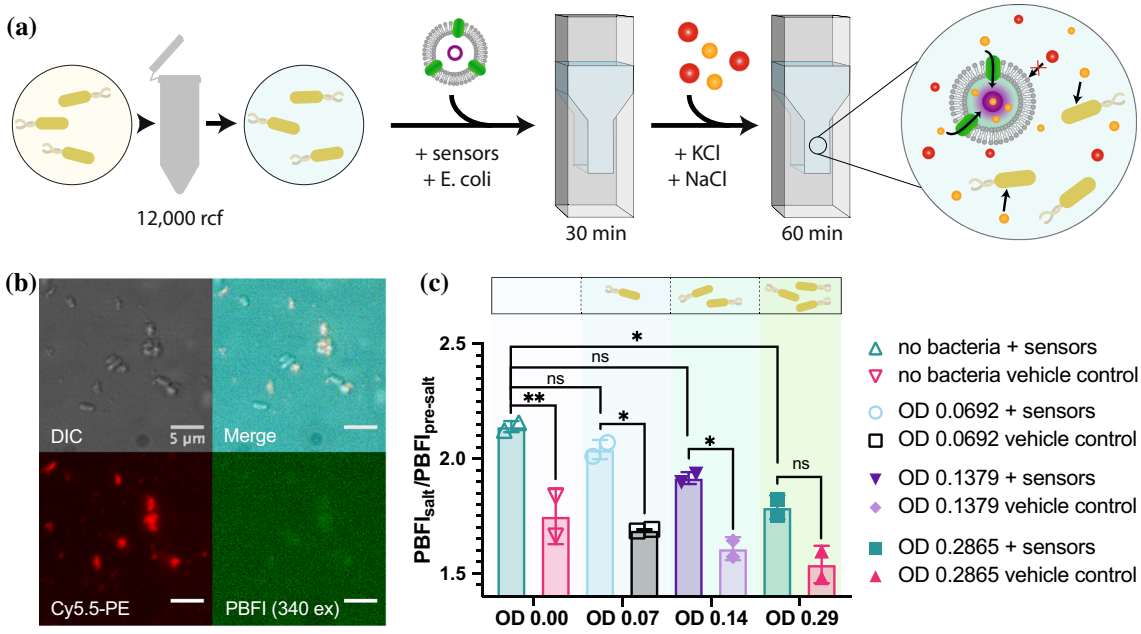

FIGURE 5. Vesicles detect variations in [K+] in the presence of increasing concentrations of bacteria. (a) Schematic of bacterial studies with nanosensors. First, bacteria grown in MSgg media are spun down and resuspended in equiosmolar Tris. Bacteria diluted to varying final optical densities are added to a fluorimeter cuvette with 1 mM nanosensors. Following a 30 min incubation in the absence of salt, 50 mM KCl and 150 mM NaCl are added to cuvettes. Nanosensor fluorescence was assessed via fluorimeter after 1 h incubation following salt addition. (b) Nanosensors imaged after 1 hour of co-incubation with bacteria show distinct fluorescence of Cy5.5-PE, a membrane dye, and faint localization of PBFI measured at the 340 nm excitation wavelength. Nanosensors can be observed to be intact and in solution surrounding bacterial cells. (c) Change in nanosensor fluorescence following salt addition decreases as the concentration of bacteria increases, indicating potassium uptake by bacteria. Nanosensors in the absence of bacteria exhibit a significantly higher change in fluorescence compared to nanosensors incubated with bacteria at an optical density of 0.2865. Similarly, a significant difference was observed between sensor and vehicle control conditions in the absence of bacteria, while significance between these conditions decreases as bacterial optical density increases. No significant differences were observed between any vehicle control conditions (pink, black, light purple and pink bars; ns $p > 0.05$), not shown. $N = 2$, error bars represent standard deviation. $^{**}p \leq 0.01$, $^{*}p \leq 0.05$, nonsignificant (ns) $p > 0.05$; p values generated using a Two-Way ANOVA and Tukey's Multiple Comparisons Test.

vesicles prevented the indicator from interacting with off-target cations, particularly Na^+ and Ca^{2+}, which cannot readily pass through bilayer membranes.[24] We then showed that the incorporation of the K^+-specific transporter, valinomycin, allowed the specific access of K^+ to the vesicle interior, allowing sensors to respond to increasing K^+ concentrations in the surrounding buffer. While the lipid membrane creates a physical barrier that does impact the speed of detection for these nanosensors compared to free dye, it also greatly improves the specificity of K^+ detection for this ion indicator. Finally, we were able to detect changes in K^+ concentrations in bacterial cultures in response to hyperosmotic shock, showing that changes in extracellular K^+ concentrations and bacterial uptake of K^+ can be detected. While buffer components and incubations times are important factors to consider in deployment of these nanosensors, the improved specificity, ease of use, and straightforward assembly of this platform should expand the applications of small-molecule, ion-specific sensing.

In many biological contexts in which various cations are present simultaneously, the ability to distinguish between ions of varying identities is key to understanding the role of electrolyte balance in biological functions. Nanosensors, such as the one described here, may help improve the functionality of existing technologies, namely fluorescent, small-molecule indicators, toward these applications. Vesicles, in particular, provide an exciting platform to expand the environments in which ion indicators can be used, as they can incorporate a wide variety of natural and synthetic components, can be engineered to be highly biocompatible, and can retain stability in a range of extravesicular environments.[3] They might also serve as a "handle" to concentrate and retain these signals in a localized environment, something difficult to achieve with free dye alone. Understanding how vesicle encapsulation balances the kinetics and signal of ion indicators will be an important next step for investigation. Drawing from a diverse toolbox of naturally-derived membrane transporters, synthetic and naturally-derived lipids, and water-soluble small mo-

lecule indicators, a variety of sensors could be developed which allow for the specific detection of small molecule targets—even in the presence of similar analytes.

MATERIALS AND METHODS

Materials

DOPC (18:1 (Δ9) 1,2-dioleyoyl-sn-glycero-3-phosphocholine, 25 mg/mL in chloroform) was obtained from Avanti Polar Lipids, Inc. PBFI Tetraamonium Salt (4,4'-[1,4,10,13-Tetraoxa-7,16-diazacyclooctadecane-7,16-diylbis(5-methoxy-6,2-benzofurandiyl)]bis-1,3-benzenedicarboxylic acid), Tris buffer (pH 7), KCl, $MgCl_2$, $CaCl_2$, and NaCl were obtained from Thermo Fisher. Valinomycin Ionophore and Sepharose 4B were obtained from Sigma-Aldrich. MSgg media was prepared as described in supplemental methods, all buffer components were obtained from Sigma Aldrich. Size exclusion chromatography columns were obtained from BioRad. BL21 bacteria was obtained from New England Biolabs.

Vesicle Preparation

Small unilamellar vesicles were prepared through thin film hydration as described by Boyd *et al.*[4] Briefly, DOPC in chloroform was dried down in glass vials under nitrogen gas and placed under vacuum pressure overnight. Lipid films were hydrated immediately or were frozen at -20°C and used within one week. Films were rehydrated overnight at 4°C with Tris buffer (100 mM for specificity studies, 200 mM for bacterial studies) containing 0.5 mM PBFI dye to a final concentration of 20 or 40 mM lipid. Films were vortexed briefly to form vesicles, then extruded through 100 nm polycarbonate filters (Avanti Polar Lipids, Inc.) to 7 passes. Unencapsulated PBFI dye was removed by purifying vesicles using size exclusion chromatography, and vesicle fractions were collected using an FC 204 Fraction Collector (Gilson). Size characterization was performed through dynamic light scattering on a Keck-II Zetasizer. Vesicles were diluted in buffer to a final concentration of 100 μM; vesicle samples were run in triplicate and the intensity mean was taken as the average diameter size.

A 100 uM valinomycin stock solution was made in 100 mM Tris + 1% DMSO and added to purified vesicles at various mol %s (0, 0.1, 0.2); vesicles were then incubated for >30 min at room temperature to allow for ionophore insertion. Control vesicles were prepared by adding the same volume of 100 mM Tris + 1% DMSO without valinomycin. Vesicles were prepared with valinomycin in triplicate.

For reversibility studies, DOPC vesicles were prepared at a concentration of 40 mM and, before purification, were incubated with either 0.2 mol% valinomycin or the corresponding volume of DMSO buffer for 30 min. Vesicles were then incubated in either 0 mM K^+ or 100 mM K^+ for 1 hour. Following salt incubation, samples were purified through size exclusion columns containing either 100 mM Tris running buffer or 100 mM Tris + 100 mM K^+ running buffer. Following purification, samples were incubated at room temperature for 1 h before reading PBFI fluorescence.

For calcein release assays, vesicles were prepared by hydrating lipid films as described above with 100 mM Tris buffer containing 20 mM Calcein dye. Vesicles were incubated at 37°C for 24 hrs, vortexed briefly, then extruded through 100 nm polycarbonate filters (Avanti Polar Lipids, Inc.) to 7 passes. Unencapsulated Calcein dye was removed by purifying vesicles using size exclusion chromatography, and vesicle fractions were collected using an FC 204 Fraction Collector (Gilson). Valinomycin was incorporated into vesicle membranes as described above.

Sensor Characterization

Vesicles were incubated in 384 well plates or 0.5 mL cuvettes with varying salt buffers and monitored for changes in PBFI fluorescence ratio. Final vesicle concentration was 1 mM during incubation, and salt conditions were varied between 0 and 100 mM in 100 mM Tris buffer pH 7. PBFI fluorescence in vesicles was measured either over time for kinetic scans or following 1 hour buffer incubation. For free dye characterization, PBFI was added to buffers with varying salt content at a concentration of 0.0125 mM to obtain a similar overall dye concentration to that of the vesicle samples following purification and dilution. For kinetic studies, 1 μL 10% TritonX-100 was added per 30 μL volume and fluorescence was monitored to determine maximum PBFI ratio.

For vesicle stability assays, Calcein fluorescence was monitored at an excitation of 495 nm and emission at 515 nm. Following vesicle incubation in buffers with increasing KCl concentration, 1 μL 10% TritonX-100 was added per 40 μL volume and incubated for 30 min to lyse vesicles and determine the fluorescence associated with 100% dye release. The stability of the vesicles was assessed by evaluating the calcein leakage with each valinomycin concentration relative to the control.

Statistical analysis and model fitting were conducted with GraphPad Prism. Results were analyzed *via* Two-Way ANOVA using Tukey's Multiple Comparisons

Test to assess significance between conditions. P values are reported as: $****p \leq 0.0001$, $***p \leq 0.001$, $**p \leq 0.01$, $*p \leq 0.05$, nonsignificant (ns) $p > 0.05$.

Fluorescence Spectroscopy

PBFI fluorescence was measured by taking spectral scans monitoring emission intensity at 505 nm with excitation wavelengths ranging from 320 to 400 nm. PBFI ratios were calculated by taking the fluorescence emission at 505 nm when excited at 340 nm divided by the fluorescence emission at 505 nm when excited at 380 nm:

$$Ratio340/380 = 505Em.Intensity_{340ex}/505Em.Intensity_{380ex}$$

Spectroscopic measurements were collected on a SpectraMax i3x plate reader (Molecular Devices) and a Cary Eclipse Fluorescence Spectrophotometer (Agilent Technologies).

Bacterial Studies

Wild type BL21 *E. coli* were grown overnight in MSgg media (see SI) at 37°C with shaking. Bacteria were centrifuged at 12,000 rcf for 2 minutes to form a pellet, MSgg supernatant was removed, and bacteria were re-suspended in equiosmolar Tris (326 mmol/kg, measured using a Wescor Vapro 5520 vapor pressure osmometer). Vesicles were prepared with 0.2 mol% Valinomycin (or an equal volume of DMSO) and 0.5 mM PBFI as described above. Vesicles were mixed in a cuvette with buffer to a final concentration of 1 mM, and bacteria were added in three separate concentrations, keeping final volume constant. Final OD was measured on a Cary UV Vis Spectrophotometer, zeroed to vesicles in buffer. PBFI excitation spectra from 330 to 390 nm were monitored for 30 min in the absence of any salt on a Cary Eclipse Fluorescence Spectrophotometer with high PMT sensitivity at an emission of 505 nm. After a 30 minute incubation of vesicles and bacteria, 50 mM KCl and 150 mM NaCl was added to each cuvette and mixed via pipetting. Fluorescence was monitored for 60 minutes following salt addition. To account for differences in optical densities, final PBFI ratios were assessed by dividing the final fluorescence ratio after salt addition by the initial fluorescence ratio with vesicles and bacteria only.

Samples were imaged on a Nikon Ti2 microscope in the presence of WT BL21 to assess stability and localization. Vesicles were prepared as described but with the addition of 0.1 mol% of Cy5.5-PE, a membrane dye. Vesicles and bacteria were mixed together in buffer and allowed to incubate for 1 h. Images were taken with filters for DIC, Cy5.5-PE (650 nm excitation, 720 nm emission) and the 340 nm excitation of PBFI (350 nm excitation, 525 nm emission).

SUPPLEMENTARY INFORMATION

The online version contains supplementary material available at https://doi.org/10.1007/s12195-021-00688-7.

ACKNOWLEDGMENTS

This work was supported by the Cornew Innovation Award from the Chemistry of Life Processes Institute at Northwestern University (to NPK) and the National Science Foundation (CBET-1844219 and CBET-1844336 to NPK). MAB was supported by the National Defense Science and Engineering Graduate Fellowship through the Department of Defense. AMD and NRC were assisted by a grant from the Undergraduate Research Grant Program, which is administered by Northwestern University' s Office of Undergraduate Research, and by a grant from Northwestern's Biomedical Engineering Department.

CONFLICT OF INTEREST

Margrethe Boyd, Anna Davis, Nora Chambers, Peter Tran, Arthur Prindle, and Neha P. Kamat declare that they have no conflicts of interest.

ETHICAL APPROVAL

No animal or human studies were performed in this work.

REFERENCES

[1]Bazzigaluppi, P., S. Dufour, and P. L. Carlen. Wide field fluorescent imaging of extracellular spatiotemporal potassium dynamics *in vivo*. *Neuroimage*, 104:110–116, 2015.
[2]Bischof, H., *et al.* Novel genetically encoded fluorescent probes enable real-time detection of potassium *in vitro* and *in vivo*. *Nat. Commun.* 8:1–12, 2017.
[3]Boyd, M. A., and N. P. Kamat. Designing artificial cells towards a new generation of biosensors. *Trends Biotechnol.* In Press, 2020.
[4]Boyd, M. A., and N. P. Kamat. Visualizing tension and growth in model membranes using optical dyes. *Biophys. J.*, 115:1307–1315, 2018.
[5]Cayley, S., and M. T. Record. Roles of cytoplasmic osmolytes, water, and crowding in the response of escherichia

coli to osmotic stress: biophysical basis of osmoprotection by glycine betaine. *Biochemistry* 42:12596–12609, 2003.
[6]Cheng, C. J., E. Kuo, and C. L. Huang. Extracellular potassium homeostasis: insights from hypokalemic periodic paralysis. *Semin. Nephrol.* 33:237–247, 2013.
[7]Dinnbier, U., E. Limpinsel, R. Schmid, and E. P. Bakker. Transient accumulation of potassium glutamate and its replacement by trehalose during adaptation of growing cells of Escherichia coli K-12 to elevated sodium chloride concentrations. *Arch. Microbiol.* 150:348–357, 1988.
[8]Dufour, S., P. Dufour, O. Chever, R. Vallée, and F. Amzica. *In vivo* simultaneous intra- and extracellular potassium recordings using a micro-optrode. *J. Neurosci. Methods* 194:206–217, 2011.
[9]Eil, R., *et al*. Ionic immune suppression within the tumour microenvironment limits T cell effector function. *Nature* 537:539–543, 2016.
[10]Filosa, J. A., *et al*. Local potassium signaling couples neuronal activity to vasodilation in the brain. *Nat. Neurosci.* 9:1397–1403, 2006.
[11]Halperin, M. L., and K. S. Kamel. Potassium. *Lancet* 352:135–140, 1998.
[12]He, H., M. A. Mortellaro, M. J. P. Leiner, R. J. Fraatz, and J. K. Tusa. A fluorescent sensor with high selectivity and sensitivity for potassium in water. *J. Am. Chem. Soc.* 125:1468–1469, 2003.
[13]Kasner, S. E., and M. B. Ganz. Regulation of intracellular potassium in mesangial cells: A fluorescence analysis using the dye, PBFI. *Am. J. Physiol. Ren. Fluid Electrolyte Physiol.* 262:F462–F467, 1992.
[14]Kozoriz, M. G., J. Church, M. A. Ozog, C. C. Naus, and C. Krebs. Temporary sequestration of potassium by mitochondria in astrocytes. *J. Biol. Chem.* 285:31107–31119, 2010.
[15]Kubitschek, H. E., M. L. Freedman, and S. Silver. Potassium uptake in synchronous and synchronized cultures of Escherichia coli. *Biophys. J.* 11:787–797, 1971.
[16]Li, C., G. L. Law, and W. T. Wong. Luminescent $Tb3^+$ complex with pendant crown ether showing dual-component recognition of H^+ and K^+ at multiple pH windows. *Org. Lett.* 6:4841–4844, 2004.
[17]Liu, J., *et al*. A highly sensitive and selective nanosensor for near-infrared potassium imaging. *Sci. Adv.* 6:1–11, 2020.
[18]Liu, J., *et al*. A sensitive and specific nanosensor for monitoring extracellular potassium levels in the brain. *Nat. Nanotechnol.* 15:321–330, 2020.
[19]Lomora, M., F. Itel, I. A. Dinu, and C. G. Palivan. Selective ion-permeable membranes by insertion of biopores into polymersomes. *Phys. Chem. Chem. Phys.* 17:15538–15546, 2015.
[20]McLaggan, D., J. Naprstek, E. T. Buurman, and W. Epstein. Interdependence of K^+ and glutamate accumulation during osmotic adaptation of *Escherichia coli*. *J. Biol. Chem.* 269:1911–1917, 1994.
[21]Meury, J., A. Robin, and P. Monnier-Champiex. Turgor-controlled K^+ fluxes and their pathways in *Escherichia coli*. *Eur. J. Biochem* 151:613–619, 1985.
[22]Meuwis, K., N. Boens, F. C. De Schryver, J. Gallay, and M. Vincent. Photophysics of the fluorescent K^+ indicator PBFI. *Biophys. J.* 68:2469–2473, 1995.
[23]Minta, A., and R. Y. Tsien. Fluorescent indicators for cytosolic sodium. *J. Biol. Chem.* 264:19449–19457, 1989.
[24]Monnard, P. A., and D. W. Deamer. Membrane self-assembly processes: steps toward the first cellular life. *Anat. Rec.* 268:196–207, 2002.
[25]Mueller, P., and D. O. Rudin. Development of K^+Na^+ discrimination in experimental bimolecular lipid membranes by macrocyclic antibiotics. *Biochem. Biophys. Res. Commun.* 26:398–404, 1967.
[26]Newsom-Davis, J., *et al*. Autoimmune disorders of neuronal potassium channels. *Ann. N. Y. Acad. Sci.* 998:202–210, 2003.
[27]Padmawar, P., X. Yao, O. Bloch, G. T. Manley, and A. S. Verkman. K^+ waves in brain cortex visualized using a long-wavelength K^+-sensing fluorescent indicator. *Nat. Methods* 2:825–827, 2005.
[28]Palmer, B. F. Regulation Of Potassium Homeostasis. *Clin. J. Am. Soc. Nephrol.* 10:1050–1060, 2014.
[29]Prindle, A., J. Liu, M. Asally, S. Ly, J. Garcia-Ojalvo, and G. M. Süel. Ion channels enable electrical communication in bacterial communities. *Nature* 527:59–63, 2015.
[30]Rana, P. S., *et al*. Calibration and characterization of intracellular Asante Potassium Green probes, APG-2 and APG-4. *Anal. Biochem.* 567:8–13, 2019.
[31]Rimmele, T. S., and J. Y. Chatton. A novel optical intracellular imaging approach for potassium dynamics in astrocytes. *PLoS ONE* 9:e109243, 2014.
[32]Sica, D. A., A. D. Struthers, W. C. Cushman, M. Wood, J. S. Banas, and M. Epstein. Importance of potassium in cardiovascular disease. *J. Clin. Hypertens.* 4:198–206, 2002.
[33]Steller, L., M. Kreir, and R. Salzer. Natural and artificial ion channels for biosensing platforms. *Anal. Bioanal. Chem.* 402:209–230, 2012.
[34]Su, Z. F., X. Q. Ran, J. J. Leitch, A. L. Schwan, R. Faragher, and J. Lipkowski. How valinomycin ionophores enter and transport K^+ across model lipid bilayer membranes. *Langmuir* 35:16935–16943, 2019.
[35]Szatmári, D., *et al*. Intracellular ion concentrations and cation-dependent remodelling of bacterial MreB assemblies. *Sci. Rep.* 10:12002, 2020.
[36]van de Velde, L., E. d'Angremont, and W. Olthuis. Solid contact potassium selective electrodes for biomedical applications—a review. *Talanta* 160:56–65, 2016.
[37]Yellen, G. The voltage-gated potassium channels and their relatives. *Nature*. 419:35–42, 2002.
[38]Zhou, X., F. Su, Y. Tian, C. Youngbull, R. H. Johnson, and D. R. Meldrum. A new highly selective fluorescent K^+ sensor. *J. Am. Chem. Soc.* 133:18530–18533, 2011.

Publisher's Note Springer Nature remains neutral with regard to jurisdictional claims in published maps and institutional affiliations.